Photodissociation of $ClONO_2$: 2. Time-Resolved Absorption Studies of Product Quantum Yields

R. J. Yokelson,[†] James B. Burkholder,* R. W. Fox,[‡] and A. R. Ravishankara[§]

Aeronomy Laboratory, NOAA, 325 Broadway, Boulder, Colorado 80303, and Cooperative Institute for Research in Environmental Sciences, University of Colorado, Boulder, Colorado 80309

Received: March 4, 1997; In Final Form: May 22, 1997[⊗]

The quantum yield for NO_3 production in the UV photolysis of $ClONO_2$ was measured *via* transient 661.9 nm absorption of NO_3 following pulsed laser photolysis and was found to be 0.93 ± 0.24 at 352.5 nm, 0.67 ± 0.09 at 308.15 nm, 0.60 ± 0.09 at 248.25 nm, and 0.18 ± 0.04 at 193 nm. The Cl atom quantum yield was measured by reacting Cl with $ClONO_2$ to produce NO_3 through the reaction $Cl + ClONO_2 \rightarrow Cl_2 + NO_3$ and was found to be 0.73 ± 0.14 at 308.15 nm, 0.60 ± 0.12 at 248.25 nm, and 0.45 ± 0.08 at 193 nm. The estimated O atom yields were <0.4 at 248.25 nm and <0.9 at 193 nm. Quoted error limits are at the 95% confidence level and include estimated systematic errors. The results from this study are compared with those from previous studies. On the basis of this work and that of Goldfarb *et al.* (Goldfarb, L.; Schmoltner, A.-M.; Gilles, M. K.; Burkholder, J. B.; Ravishankara, A. R. *J. Phys. Chem.* **1997**, *101*, 6658.), it is concluded that Cl and NO_3 are the major products in the photolysis of $ClONO_2$ at wavelengths important in the stratosphere and that the total quantum yield for dissociation is close to 1. The implications of these findings to stratospheric chemistry are discussed.

Introduction

In the companion paper,[1] we have described the significance of $ClONO_2$ in the chemistry of the stratosphere and, in particular, the unique way it couples chlorine and nitrogen oxides. We also detailed the role of $ClONO_2$ photolysis in partitioning of chlorine compounds between inactive and reactive forms and in the catalytic cycle involving $ClONO_2$ which destroys ozone in the stratosphere. In that paper, we described our determinations of the quantum yields for the production of O, Cl, and ClO in the photolysis of $ClONO_2$ at 193, 222, 248, and 308 nm.

As noted in the companion paper, the energetically accessible photodissociation channels for $ClONO_2$ at wavelengths longer than 200 nm are

$$ClONO_2 \xrightarrow{h\nu} ClO + NO_2 \qquad \lambda < 1066\ nm \qquad (1a)$$

$$\xrightarrow{h\nu} Cl + NO_3 \qquad \lambda < 697\ nm \qquad (1b)$$

$$\xrightarrow{h\nu} Cl + NO + O_2 \qquad \lambda < 636\ nm \qquad (1c)$$

$$\xrightarrow{h\nu} ClONO + O \qquad \lambda < 426\ nm \qquad (1d)$$

$$\xrightarrow{h\nu} Cl + NO_2 + O \qquad \lambda < 314\ nm \qquad (1e)$$

$$\xrightarrow{h\nu} ClO + NO + O \qquad \lambda < 286\ nm \qquad (1f)$$

$$\xrightarrow{h\nu} ClONO + O(^1D) \qquad \lambda < 254\ nm \qquad (1g)$$

$$\xrightarrow{h\nu} Cl + NO_2 + O(^1D) \qquad \lambda < 210\ nm \qquad (1h)$$

By measuring the quantum yields for O and Cl atoms and ClO and NO_3 molecules, all the photolysis channels of importance to the atmosphere (1a−e) can be characterized. Recently, Nickolaisen *et al.*[2] have reported that the quantum yield for the dissociation of $ClONO_2$ in broad-band photolysis at wavelengths greater than 300 nm decreases with increasing pressure. We have not measured the quantum yields for the loss of $ClONO_2$, except at 193 nm. However, determinations of the absolute quantum yields of various products at stratospheric pressures will shed light on the possible quenching of excited $ClONO_2$.

In this study, we report absolute quantum yields at 193, 248, 308, and 351 nm for the production of NO_3 in $ClONO_2$ photolysis. These quantum yields were measured using pulsed laser photolysis-transient absorption of NO_3 at 661.9 nm and quantified using actinometric methods. In addition to NO_3, Cl atom quantum yields were obtained relative to that for NO_3 at 193, 248, and 308 nm by quantitative conversion of Cl to NO_3 by the reaction

$$Cl + ClONO_2 \rightarrow Cl_2 + NO_3 \qquad (2)$$

Oxygen atom quantum yields were estimated indirectly at 193 and 248 nm by conversion to O_3:

$$O + O_2 \xrightarrow{M} O_3 \qquad (3)$$

In this paper, we compare the results from our two studies with those from previous investigations and discuss the significance of our findings to the chemistry of the stratosphere.

Experimental Section

The experiments described here were designed to measure the absolute quantum yields of NO_3 using transient absorption at 661.9 nm. The quantum yields of $Cl(^2P)$ at 193, 248, and 308 nm were also derived by observing the NO_3 radical formed as a product of the reaction 2. At 193 and 248 nm, the quantum yields of O atoms (sum of $O(^1D)$ and $O(^3P)$ quantum yields) were estimated by converting O atoms to O_3 *via* reaction 3 and measuring the resultant O_3 by UV absorption. Any $O(^1D)$ that was produced was rapidly quenched to $O(^3P)$. In this study, we did not differentiate between $O(^1D)$ and $O(^3P)$.

[†] Present address: Department of Chemistry, University of Montana, Missoula, MT 59812.

* Author to whom correspondence should be addressed: NOAA R/E/AL2, 325 Broadway, Boulder, CO 80303.

[‡] At National Institute of Standards and Technology, Time and Frequency Division, 325 Broadway, Boulder, CO 80303.

[§] Also affiliated with the Department of Chemistry and Biochemistry, University of Colorado, Boulder, CO 80309.

[⊗] Abstract published in *Advance ACS Abstracts,* July 15, 1997.

S1089-5639(97)00819-0 CCC: $14.00

TABLE 1: Absorption Cross Sections of Various Compounds at 298 K[a]

	Wavelength, nm											
compd	193	216	220	248.25	253.7	255.5	278	308.15	330	352.5	661.9	ref
Cl_2									0.261	0.181		19
O_3	0.434	1.02	1.78	10.76	11.6	11.7	4.67	0.134				12
ClO					4.04							7
$ClONO_2$	4.64	3.45	3.32	0.616				0.0181		0.00216		20
NO_3											22.3	5

[a] Data from the same references were used when the cross sections at other temperatures were needed. All absorption cross sections in units of 10^{-18} cm^2 $molecule^{-1}$.

The determination of the quantum yield of a photoproduct requires measuring its concentration and the concentration of the photolyte that absorbed light. The concentration of the photoproduct was directly measured during these experiments. The concentration of the photolyte that absorbed light is, in general, difficult to measure. If a large fraction of the molecules absorbed light and dissociated, the loss of the photolyte may be measurable. We were able to directly measure the loss of $ClONO_2$ in the 193 nm photolysis, but at other wavelengths, actinometry was necessary. The concentration of the photolyte that absorbed light was calculated using the absorption cross section of the photolyte and the photon fluence at the photolysis wavelength. The absorption cross sections were taken from the literature and are listed in Table 1. Determination of the laser fluence, actinometry, is described below.

The apparatus used in this investigation has been previously described in detail.[3−5] Detection of NO_3 by using a tunable diode laser in a pulsed photolysis system is also described in a previous publication.[4] Due to the small absorption cross sections of $ClONO_2$ at $\lambda > 290$ nm, the wavelengths important for atmospheric photolysis, good sensitivity for NO_3 detection was essential to directly measure NO_3 formed in $ClONO_2$ photolysis. The long-path absorption method using a tunable diode laser provided the required sensitivity.

For each photolysis wavelength, the optical alignment varied slightly and different actinometric methods were used to determine the photon fluence. In this section we will describe (1) the apparatus, procedures, and data acquisition methods for measuring $ClONO_2$ loss, NO_3 production, and O_3 generation in the presence of O_2, (2) the actinometric methods used to quantify the photolysis laser fluence, and (3) the preparation and handling of labile compounds.

The apparatus consisted of three basic components: (1) a long-path absorption cell (optical path length = 91 cm), (2) excimer lasers for pulsed photolysis, and (3) UV−vis probe beams and their detectors for measuring photolyte concentration and monitoring the temporal evolution of photoproducts. The jacketed 30 mm i.d. absorption cell was made of Pyrex, and its temperature was regulated by circulating methanol from a temperature-controlled bath through the jacket.

The use of a diode array spectrometer in this apparatus is described elsewhere.[6,7] For the present study, a D_2 lamp, a quartz−halogen lamp, and a diode laser were used as light sources for spectral and single wavelength measurements. One of these three probe beams was passed through the absorption cell at a time. Kinematically mounted mirrors allowed quick and reproducible switching between the different probe beams. A 661.9 nm diode laser, single mode with 0.5 to 2 mW output, was used to measure NO_3 transient absorption signals. Apertures were used to insure good overlap between the collimated D_2 and quartz−halogen probe beams and the copropagated excimer laser beam. The collimated output of the diode laser (0.4 mm × 1.2 mm) was significantly narrower than the cross-sectional area of the excimer photolysis beam. The diode laser beam was realigned periodically to sample different regions of the excimer laser beam path through the cell; the measured NO_3 yields were unaltered, indicating good homogeneity of the excimer laser beam. The probe beams exiting the absorption cell were directed into a 0.25 m monochromator with a PMT detector, a photodiode, or a 0.28 m spectrograph equipped with a diode array detector.

The diode array spectrometer was used to measure the concentrations of $ClONO_2$, O_3, Cl_2, and OClO in the absorption cell before and after photolysis. In one experiment, it was used to measure NO_3 produced by $ClONO_2$ photolysis. It was also used to measure the wavelength of the diode laser. A 150 μm entrance slit, which resulted in a wavelength resolution of ∼0.6 nm, was used for all concentration measurements. An electromechanical shutter, placed directly in front of the entrance slit, opened after the photolysis laser was fired and, thus, prevented exposure of the array to the excimer radiation. This configuration was used to measure changes in the $ClONO_2$ and O_3 concentrations ∼15 ms after 193 nm photolysis.[8]

The diode laser wavelength was measured after each set of experiments using the diode array spectrometer. A 10 μm entrance slit yielded a resolution of ∼0.1 nm. The wavelength scale of the spectrograph was calibrated using emission lines from a Ne lamp and was accurate to 0.1 nm. The laser wavelength was locked at the peak of the NO_3 absorption feature, 661.9 nm, by regulating the laser current (∼40 mA) and temperature (∼275 K).[9] The NO_3 absorption feature centered at 661.9 nm is broad, ∼4 nm full width at half-maximum (fwhm).[10] Its absorption cross section varies less than 3% over 0.1 nm at the peak of this band. Therefore, knowing the laser wavelength to ± 0.1 nm was adequate for our measurements. In several tests, the diode laser was tuned to wavelengths where the NO_3 cross sections were 20 and 90% of the peak value; the measured NO_3 quantum yields were unchanged.

The diode laser intensity was stable to about 1 part in 10^5 for periods of 20 ms or shorter, the time scale used in our absorption measurements. The DC level of the diode laser detector was offset by a constant current source, and the AC component was amplified and detected. This arrangement enabled us to measure absorbances at the shot noise level of the diode laser. On the basis of a detectable absorbance of $A = 1 \times 10^{-5}$ at a signal to noise ratio of 1, and the NO_3 absorption cross section, 2.23×10^{-17} cm^2 at 661.9 nm,[5] we estimate our NO_3 detection limit to be 5×10^9 molecule cm^{-3} per laser pulse.

The diode laser system was sensitive to optical feedback (back reflectance) and was also unstable if perturbed by the excimer laser radiation. The intensity of the excimer radiation getting to the diode laser and its detector was attenuated by many orders of magnitude by using a stack of attenuators, dichroic mirrors, and colored glass filters. With such an optical arrangement, the diode laser and its detection system recovered completely within 20 μs after the excimer pulse was fired.

The monochromator/PMT system was used to measure transient UV absorption signals of O_3 at 254 nm using the procedures described previously.[3] All monochromator measurements were made using 250 μm slits, which resulted in a wavelength resolution of ~1.6 nm fwhm.

The signals from both the diode laser detector and the PMT detection systems were sent to a transient digitizer for digitization and signal averaging. Data acquisition was initiated approximately 1 ms before the excimer laser fired to provide a baseline from which changes in absorbance could be calculated. Transient absorption profiles for analysis were obtained by coadding signals from 10 to 100 laser shots.

Excimer Laser Wavelengths. The excimer wavelengths used in this study are nominally 193 nm (ArF), 248 nm (KrF), 308 nm (XeCl), and 351 nm (KrF). However, the 308 and 351 nm excimer laser outputs consist of two transitions separated by as much as 2 nm. The absorption spectra of $ClONO_2$, O_3, and Cl_2 are not structured, but change slightly over the small wavelength region covered by the excimer beams. The ArF and KrF lasers generate a nearly Gaussian band spanning approximately 2 nm with fwhm of 0.7 and 0.4 nm, respectively. The XeCl laser generates two closely spaced bands separated by ~0.4 nm. The output of the XeF laser consists of two sets of equally intense bands centered at ~351.3 and ~353.5 nm. Therefore, an effective single wavelength for photolysis was calculated using the fluence of the laser at small increments in wavelength over the range of the emission weighted according to the absorption cross sections of the molecule at those specific wavelengths. For example, the weighted average wavelength of the XeF laser was 352.5 nm and that of XeCl is 308.15 nm for photolyzing $ClONO_2$. The specific wavelengths of the lasers for the photolysis of $ClONO_2$ are listed in Table 1.

Materials. $ClONO_2$ was synthesized by the reaction of Cl_2O with N_2O_5,[11] stored in the dark at 195 K, and introduced into the absorption cell with a small carrier flow of He. Helium was dried by passing it through a molecular sieve trap at 77 K. The only significant impurity detectable by UV absorption in the $ClONO_2$ sample was OClO, 0.006%. The NO_2 impurity level was estimated to be <0.06%. O_3 prepared by using a commercial ozonizer was stored on silica gel at 195 K and introduced into the absorption cell using a carrier flow of N_2. N_2 (UHP, 99.9995%), O_2(UHP, 99.99%), and C_2H_6 (RP, 99.99%) were used as supplied. The pressure in the absorption cell was measured with a 1000 Torr (1 Torr = 133.3 Pa) capacitance manometer. All gases were mixed before they entered the absorption cell. The linear flow velocity of the gases in the absorption cell was normally 10 cm s^{-1}, leading to a transit time through the absorption cell of ~10 s; the flow velocity was varied between 3 and 15 cm s^{-1} in several experiments. The photolysis lasers were normally operated at or below 0.1 Hz to insure that a fresh gas mixture was available for each laser shot. Constant concentrations of Cl_2 in the reactor were obtained by flowing a mixture of 10% electronic grade Cl_2 in He (with a low water content, <10 ppmv (ppmv: parts per million volume) through a monel cross purge and regulator assembly and a 0.003 μm particle filter. The Cl_2 concentrations measured by UV absorption were constant to better than ~2% throughout the measurements.

Results

The concentration of $ClONO_2$ that absorbed the photolysis light, $\Delta[ClONO_2]$, at 248, 308, or 352.5 nm was calculated from the equation

$$\Delta[ClONO_2] = F_\lambda \sigma_\lambda^{ClONO_2}[ClONO_2] \qquad (I)$$

where F_λ is the fluence (photons cm^{-2} $pulse^{-1}$) and $\sigma_\lambda^{ClONO_2}$ is the absorption cross section of $ClONO_2$ at wavelength λ. The fluence was measured using actinometric experiments. A suitable photolyte with a known absorption cross section and photodissociation quantum yield at the wavelength of interest was photolyzed. The change in its concentration was determined. In the case of the 193 nm photolysis, the concentration of $ClONO_2$ that was destroyed by the photolysis beam was directly measured.

The optical depths in the reactor were not identical in the actinometry and $ClONO_2$ photolysis measurements because of the differing absorption cross sections and concentrations of the molecules. The fractional attenuation of the fluence along the length of the reactor in the actinometry experiments was sometimes ~10%. The differences in the attenuation were taken into account during the data analysis. The largest correction due to this difference in attenuation was 6%.

Cl and O atoms react with $ClONO_2$ to produce NO_3 *via* reactions 2 and 4.

$$O + ClONO_2 \rightarrow ClO + NO_3 \qquad (4)$$

Therefore, if produced *via* photolysis of $ClONO_2$, O and Cl atoms can produce additional NO_3. The secondary production of NO_3 due to reactions 2 and 4 are separable in time and their contributions to NO_3 generation assessed. Alternatively, generation of NO_3 *via* the O and Cl atom reactions with $ClONO_2$ could be minimized by the addition of C_2H_6 and O_2 to the absorption cell. In this study, we used scavengers to suppress secondary reactions. O atoms were scavenged by O_2 through reaction 3. Cl atoms were scavenged by C_2H_6 through the reaction

$$Cl + C_2H_6 \rightarrow HCl + C_2H_5 \qquad (5)$$

The C_2H_5 radical produced in reaction 5 was then converted to $C_2H_5O_2$ *via* reaction with O_2,

$$C_2H_5 + O_2 + M \rightarrow C_2H_5O_2 + M \qquad (6)$$

to prevent regeneration of Cl atoms through the reaction

$$C_2H_5 + Cl_2 \rightarrow C_2H_5Cl + Cl \qquad (7)$$

The specific actinometry experiments, photoproduct measurements, and data analysis routines at each of the four wavelengths were somewhat different. Therefore, for ease of presentation, they are described separately.

352.5 nm Photolysis. To measure the laser fluence in the reactor, a mixture of Cl_2 (~3×10^{15} molecule cm^{-3}) and O_3 (~4×10^{14} molecule cm^{-3}) in ~300 Torr of N_2 was photolyzed. The absorption cross section of O_3 at 351 nm is <3×10^{-22} cm^2;[12] therefore, the concentration of O_3 that was photolyzed was <0.02% of the concentration of Cl_2 that was dissociated. Photolysis of Cl_2 yields two Cl atoms:

$$Cl_2 \xrightarrow{h\nu} 2\ Cl \qquad (8)$$

The Cl atoms reacted with O_3 to form ClO *via* the reaction

$$Cl + O_3 \rightarrow ClO + O_2 \qquad (9)$$

The measured temporal profile of the absorbance at 253.7 nm was recorded using the monochromator/PMT detection system. An example of such a profile is shown in Figure 1. The fast decrease in absorbance results from the loss of ozone due to reaction 9 even though its product, ClO, also absorbs at the

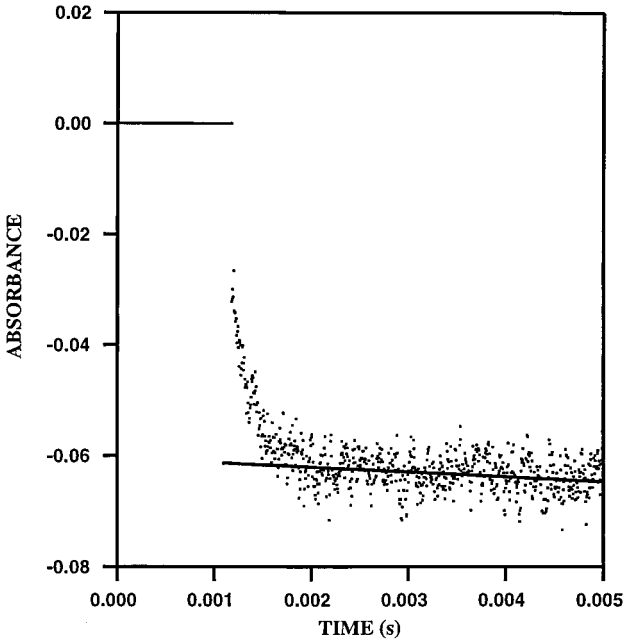

Figure 1. Representative laser fluence calibration data for 352.5 nm photolysis. The transient absorption signal was measured at 253.7 nm using the monochromator/PMT detection system. The change in absorption corresponds to the destruction of O_3 and formation of ClO (see text for details). The solid line is the fit to the data at long times, $1/A$ *vs* time, used to extrapolate the absorption signal to the time of the laser pulse, t_0. The baseline measured before the excimer laser trigger and have been averaged and set to zero in the data analysis.

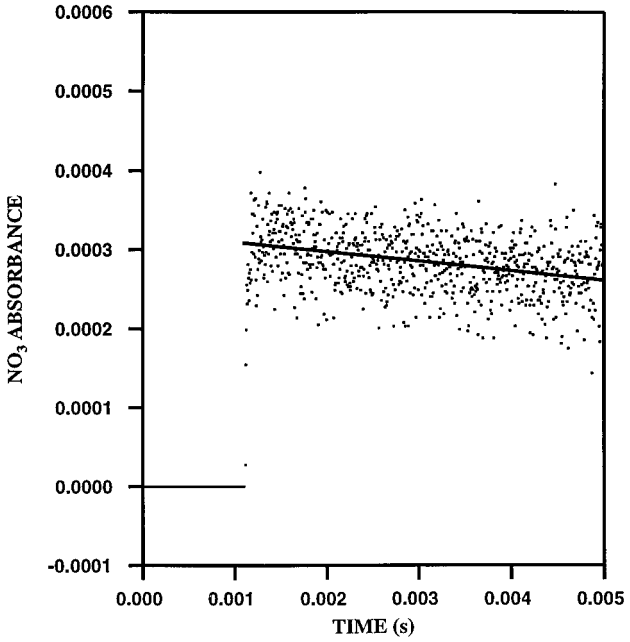

Figure 2. Representative temporal profile of NO_3 absorption at 661.9 nm following $ClONO_2$ photolysis at 352.5 nm. The $[ClONO_2]$ is 9.1 $\times$ 10^{14} molecule cm^{-3}, and the bath gas consists of 123.8 Torr of O_2 and 4.7 Torr of C_2H_6. The solid line is a fit to the data used to extrapolate the absorption signal to the time of the laser pulse t_0.

same wavelength. For each ClO that was formed, one O_3 was removed. The absorption cross section of O_3 at 253.7 nm is approximately 3 times greater than that of ClO, such that a decrease in absorbance is observed. The net change in absorbance is related to the difference between the absorption cross section of O_3 and ClO, which has been measured in our laboratory to be $\sigma_{O_3}^{253.7} - \sigma_{ClO}^{253.7} = 7.56 \times 10^{-18}$ cm^2, independent of temperature.[7] The observed temporal profile of the absorption was consistent with that expected due to the rate coefficients[10] for reaction 9 and the concentrations of O_3 that were used.

The change in absorbance reached a plateau at the completion of reaction 9. The plateau level was proportional to the amount of Cl produced *via* photolysis (*i.e.*, proportional to the laser fluence). The slow decrease in absorbance after reaching the maximum was attributed to the self reaction of ClO. At the pressures employed, the majority of the loss at short times (<20 ms) occurred *via* the formation of the dimer:

$$ClO + ClO + M \rightarrow C_2O_2 + M \qquad (10)$$

The dimer is unstable at 298 K and decomposes back to ClO with a first-order rate constant of $\sim$10 s^{-1} under our conditions. Therefore, the long-time loss of ClO and Cl_2O_2 was *via* the slower bimolecular reactions of ClO.[10] The absorption cross section of Cl_2O_2 is similar to that of ClO at 253.7 nm.[10] However, reaction 10 leads to a decrease in absorbance with time because two molecules of ClO were removed for each molecule of Cl_2O_2 that was produced. If the loss of ClO is *via* the bimolecular channel, the end products are Cl_2, O_2, and OClO,[13] which do not absorb strongly at 253.7 nm. The rate of decrease in the absorption was consistent with reaction 10 being the dominant removal pathway at short times. A least-squares fit of $1/A_\lambda$ *vs* time, where A_λ is the absorbance at 253.7 nm after reaching the maximum, was extrapolated to t_0, the time of the laser pulse, to calculate the initial concentration of the Cl, $\Delta[Cl]_0$, that was produced. Figure 1 shows such a plot and the fit. The measured $\Delta[Cl]_0$ is related to the photolysis laser fluence *via* the equation

$$F_{352.5} = \frac{\Delta[Cl]_0}{2[Cl_2]\sigma_{Cl_2}^{352.5}} \qquad (II)$$

To quantify the concentration of NO_3 that was produced, the time dependent attenuation of 661.9 nm radiation from a tunable visible diode laser was measured. Following fluence measurements using the $Cl_2/O_3/N_2$ mixtures, a $ClONO_2/N_2/C_2H_6/O_2$ mixture was flowed through the reactor. The concentration of $ClONO_2$ was measured using the diode array spectrometer. Then, the 661.9 nm beam was passed through the reactor and the mixture was photolyzed. The laser fluence and $ClONO_2$ concentration were measured before and after measuring the NO_3 yield. The fluence and the concentration were the same, within a few percent. If either had changed, the data was rejected.

Figure 2 shows a representative temporal profile of absorbance at 661.9 nm that was obtained in the photolysis of $ClONO_2$ at 352.5 nm. The attenuation of the 661.9 nm light, attributed to NO_3 absorption, is instantaneous following the laser pulse. The 661.9 nm absorbance at t_0, $A_{661.9}^0$, was obtained by extrapolation of the slowly decreasing signal back to the time of the laser pulse. The concentration of NO_3 produced, $[NO_3]_0$, was given by the relation

$$[NO_3]_0 = \frac{A_{661.9}}{\sigma_{NO_3}^{661.9} l} \qquad (III)$$

The quantum yield of NO_3 was calculated using the equation

$$\Phi_{NO3}^{352.5} = \frac{[NO_3]_0}{F_{352.5}[ClONO_2]\sigma_{ClONO_2}^{352.5}} \qquad (IV)$$

Note that the exact calculations included small corrections for

TABLE 2: Quantum Yields for Production of NO_3 in the 352.5 nm Photolysis of $ClONO_2$ and the Experimental Conditions Used

laser fluence calibration				$ClONO_2$ Photolysis						
$[Cl_2]^a$ (10^{15})	$[O_3]$ (10^{14})	P (Torr)	[Cl] (10^{13})	$P(C_2H_6)$ (Torr)	$P(O_2)$ (Torr)	P(total) (Torr)	$[ClONO_2]$ (10^{15})	$\Delta[ClONO_2]$ (10^{11})	$\Delta[NO_3]$ (10^{11})	yield of NO_3
2.72	2.65	316	8.22	1.5	124	126.4	2.04	3.83	3.72	0.971
2.72	2.65	316	8.22	2.8	121	123.9	2.08	3.91	3.62	0.926
3.36	4.37	318	10.2	2.8	121	123.7	2.08	3.98	3.36	0.846
2.84	4.34	317	8.88	2.8	121	123.8	2.07	4.05	3.22	0.796
3.12	4.36	317	9.55	4.8	127	132.3	1.87	3.60	2.70	0.751
3.12	4.36	317	9.55	4.6	128	132.3	1.87	3.59	3.04[b]	0.848
3.32	4.51	317	9.03	4.6	128	132.3	1.87	3.20	2.72[b]	0.85
3.68	4.46	315	4.33	4.9	125	130.2	1.16	0.865	0.729	0.843
2.50	4.26	322	2.78	4.6	125	130.2	1.16	0.801	0.68	0.849
2.32	4.24	322	2.67	4.6	125	130.3	1.14	0.815	0.729	0.895
2.64	4.11	324	2.92	4.6	125	130.3	1.14	0.786	0.646	0.821
3.06	4.06	316	8.92	4.7	124	128.5	0.91	1.67	1.52	0.910
3.19	4.14	319	9.42	7.5	142	149.2	0.763	1.42	1.25	0.881
3.00	4.66	317	6.99	7.6	143	150.3	0.971	1.17	1.20	1.02[c]
3.14	4.60	322	7.21	7.5	143	150.5	0.979	1.16	1.03	0.886[c]
2.90	3.69	315	6.85	7.7	143	150.9	0.819	1.21	1.32	1.09
3.71	3.70	315	12.8	8.0	142	150.5	0.774	1.69	1.43	0.848
3.24	4.26	326	10.0	7.6	144	151.2	0.859	1.45	1.62	1.12[d]
3.34	4.28	324	10.3	7.6	144	151.2	0.859	1.45	1.62	1.12[d]
3.31	3.21	318	9.33	5.7	144	149.6	0.894	1.59	1.47	0.924
3.39	4.09	318	9.13	5.7	145	151.2	1.15	1.61	1.74	1.08[c]
3.58	4.06	315	9.49	5.9	145	151.6	1.15	1.59	1.69	1.06[c]
2.74	4.06	315	7.94	5.9	145	151.6	1.15	1.74	1.69	0.97[e]
										0.93 ± 0.21[f]

[a] All concentrations are in units of molecule cm^{-3}. [b] NO_3 measured off the peak of the 662 nm band. [c] $T = 220$ K. [d] $T = 249$ K. [e] $T = 260$ K. [f] Average value.

laser attenuation. Equation A2, shown in the Appendix, involves the ratios of the measured absorbances and cross sections. Such a form has the advantage that the systematic errors arising from the uncertainties in the absorption cross sections and optical path lengths are minimized.

The measured NO_3 quantum yields are listed in Table 2 along with the parameters of the measurements. The NO_3 quantum yield measurements were repeated 16 times at room temperature to obtain an average value of $\Phi_{NO_3}^{352.5} = 0.93 \pm 0.21$. The quoted uncertainty is the 2σ standard deviation of the mean. The NO_3 quantum yield was independent of the initial $[ClONO_2]$, varied over a factor of 3, and excimer laser fluence, varied over a factor of 3. Seven measurements were also made at temperatures between 220−295 K. The results from these measurements are also listed in Table 2. The reduced temperature measurements give an average NO_3 quantum yield of 1.04 ± 0.16. Although this value is slightly higher than the room temperature results, the difference is not statistically significant.

Impurities in the $ClONO_2$ sample, namely, NO_2, OClO, and Cl_2, cannot contribute to the primary yield of NO_3. However, they may contribute to the NO_3 produced *via* secondary reactions and, therefore, their contributions to the measured quantum yields were evaluated. They are included as uncertainties in the quoted quantum yields.

The only significant impurity was Cl_2. Its absorption cross section at 352.5 nm is more than 80 times larger than that of $ClONO_2$. Therefore, even though Cl_2 was undetectable by UV absorption, < 0.5%, in our $ClONO_2$ sample, it could contribute significantly to the amount of Cl atoms that are produced. Experiments, in which Cl atoms were not scavenged (*i.e.*, when $[C_2H_6] = 0$), showed increases in NO_3 signal with time after the initial (direct) production from photolysis. The rate of the increase in NO_3 was consistent with the rate of coefficient[10] for reaction 2 and the concentration of $ClONO_2$ that was used. Analysis of the subsequent production, relative to the initial production from photolysis if $ClONO_2$, showed that the Cl atom quantum yield implied by the increase corresponded to a value of ~1.1, slightly greater than unity. This indicates contributions to the Cl atom signal from sources other than $ClONO_2$. The presence of Cl_2 impurity prevented us from quantifying the yield of Cl atoms in $ClONO_2$ photolysis at 352.5 nm using the secondary production of NO_3.

308 nm Photolysis. To measure the laser fluence at 308 nm, a mixture of O_3 ($(3-8) \times 10^{14}$ molecule cm^{-3}) in 200−320 Torr of N_2 was photolyzed and the change in absorption at 253.7 nm, the peak of O_3 absorption spectrum, was measured as a function of time using the monochromator/PM tube combination. Photolysis of O_3 at 308 nm produces both $O(^1D)$ and $O(^3P)$

$$O_3 \xrightarrow{h\nu\ (308\ nm)} O(^1D) + O_2(^1\Delta) \qquad (11a)$$

$$\xrightarrow{h\nu\ (308\ nm)} O(^3P) + O_2(^1\Sigma) \qquad (11b)$$

$O(^1D)$ was rapidly (>99% in <25 ns) quenched by N_2 to $O(^3P)$. The reaction of $O(^3P)$ and $O_2(^1\Delta)$ with O_3

$$O(^3P) + O_3 \rightarrow 2\ O_2 \qquad (12)$$

$$O_2(^1\Delta) + O_3 \rightarrow O(^3P) + 2\ O_2 \qquad (13)$$

are very slow, $k_{12} = 8 \times 10^{-15}$ and $k_{13} = 3.8 \times 10^{-15}$ cm^3 $molecule^{-1}$ s^{-1} at 298 K,[10] such that the changes in O_3 during the first 10 ms is solely due to photolysis. The measured change in O_3 concentration, $\Delta[O_3]$, is related to the laser fluence at 308 nm *via* the equation

$$F_{308} = \frac{\Delta[O_3]}{[O_3]\sigma_{O_3}^{308}} \qquad (V)$$

Following the fluence measurements, NO_3 production from $ClONO_2$ photolysis was measured using the diode laser absorption. Figure 3 shows a representative NO_3 temporal profile

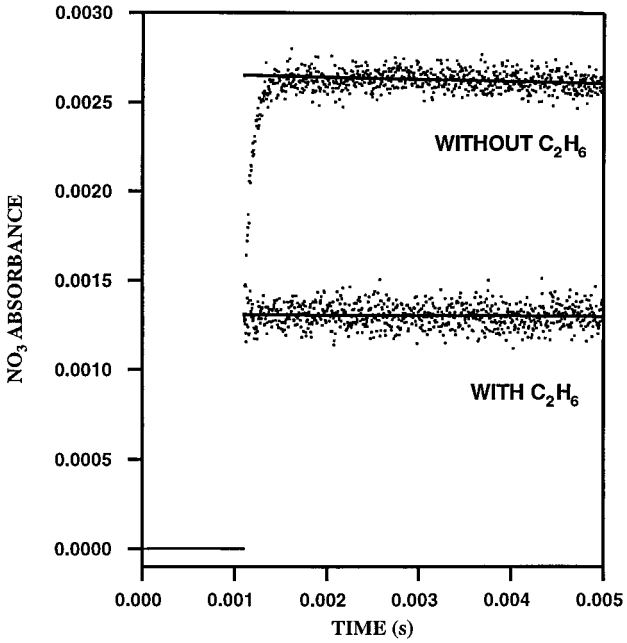

Figure 3. Typical NO_3 temporal profile following 308 nm photolysis of $ClONO_2$ in the presence of O_2, 158.7 Torr, with and without 8.4 Torr of C_2H_6. The solid lines are fits to the data used to extrapolate the absorption signal to the time of the laser pulse t_0.

obtained following 308 nm photolysis of $ClONO_2$ in the presence of O_2 and C_2H_6. Such profiles were extrapolated to the time at which the laser fired, t_0, to determine the initial concentration of NO_3 produced from the photolysis. The calculation of the quantum yield was similar to that for 352.5 nm. The obtained values of the NO_3 quantum yield are given in Table 3. Five measurements were made with NO_3 quantum yield values in the range 0.65 to 0.71 with an average of 0.67 $\pm$ 0.04. The quoted error is two standard deviations of the mean.

The Cl atom yield was measured indirectly by photolyzing a mixture of $ClONO_2$, O_2, and N_2 and measuring the increase in NO_3 produced subsequent to its direct production *via* reaction 2. Figure 3 shows the NO_3 temporal profile measured in such an experiment. The slow decrease in NO_3 signal, with a first-order rate constant of $\sim$5 s^{-1}, after reaching a maximum, is discussed for the case of 352 nm experiments. The maximum value of the 661.9 absorbance was used to calculate the sum of the NO_3 and Cl channels. The maximum NO_3 concentration can be attributed to the sum of the yields if Cl atoms are produced only *via* photolysis of $ClONO_2$ since all Cl atoms react only with $ClONO_2$. If a significant concentration of Cl atoms are produced *via* photolysis of an impurity, for example, Cl_2, this equality will not hold. The sum of the yields of NO_3 and Cl were measured three times to obtain an average value of 1.40 $\pm$ 0.10.

Alternatively, the temporal profiles of NO_3 measured in the absence of C_2H_6 were analyzed using an analytical expression, which accounts for the initial production *via* photolysis followed by a slower production *via* reaction.[4] The ratio of the sum of the yields (*i.e.*, due to photolysis and reaction) to that due to photolysis of $ClONO_2$ alone, $(\Phi(NO_3) + \Phi(Cl))/\Phi(NO_3)$, was calculated to be 2.04. The relative yield is independent of absorption cross sections and fluence. The only source of error in this quantity is the contribution from an impurity, such as Cl_2, which leads to generation of NO_3. The rate coefficient for reaction 2 extracted from this analysis was 9.4×10^{-12} cm^3 $molecule^{-1}$ s^{-1} in excellent agreement with the value reported in a recent study from this laboratory.[4]

248 nm Photolysis. The laser fluence at 248 nm was measured in the same way as at 308 nm. There was, however, a difference in the optical arrangements for two reasons: (1) ozone absorbs so strongly at 248 nm that we could use only small concentrations of ozone in the cell to maintain optically thin conditions. (2) The peak of the ozone absorption at 253.7 nm is too close to the wavelength of photolysis to prevent detection of the excimer beam. Therefore, instead of 253.7 nm, we used 278 nm to monitor O_3 loss. The absorption cross section of ozone at 278 is approximately 40% of that at 253.7 nm and was sufficient to accurately measure the changes in O_3

TABLE 3: Quantum Yields for Production of NO_3, Cl, and O Atoms in the 308 and 248 nm Photolysis of $ClONO_2$ and the Experimental Conditions Used

laser fluence calibration			$ClONO_2$ photolysis								
$[O_3]^a$ (10^{14})	P(total) (Torr)	[O] (10^{13})	$P(C_2H_6)$ (Torr)	$P(O_2)$ (Torr)	P(total) (Torr)	$[ClONO_2]$ (10^{15})	$\Delta[ClONO_2]$ (10^{11})	$\Delta[NO_3]$ (10^{11})	yield of NO_3	yield of Cl + yield of NO_3[b]	yield of O
						308 nm					
6.73	324	0.197	7.6	150.1	157.7	0.56	2.23	1.50	0.671		
3.01	320	0.195	7.6	159.5	167.1	1.29	11.3	7.98	0.708		
3.01	320	0.195	7.7	158.4	166.1	0.746	6.53	4.42	0.677		
7.81	218.4	0.409	8.4	158.7	167.1	1.38	9.85	6.46	0.656		
7.81	218.4	0.409	7.9	157.7	165.6	0.872	6.23	4.06	0.652		
									0.67 $\pm$ 0.04[c]		
3.01	320	0.195	0	158.9	158.9	1.39	12.2	17.7		1.45	
7.81	218.4	0.409	0	158.1	158.1	1.50	10.7	14.6		1.36	
7.81	217.1	0.412	0	156.3	156.3	0.948	6.82	9.56		1.40	
										1.40 $\pm$ 0.09[c]	
						248 nm					
2.61	300	3.08	7.5	134.4	141.9	1.34	93.0	59.1	0.636		
2.61	300	3.08	6.7	154.3	154.3	1.24	86.2	50.6	0.587		
2.61	300	3.08	17	209	228	0.858	60.3	35.5	0.589		
									0.60 $\pm$ 0.06[c]		
2.41	305	2.91	0	217	217	0.883	63.5	76.7		1.21	
2.41	305	2.91	0	217	217	0.874	62.6	74.9		1.2	
										1.2[c]	
2.41	299	4.66	0	217	217	0.883	63.5	23.5			0.37
2.46	299	4.66	0	217	217	3.60	379	103.0			0.27
											0.32[c]

[a] All concentrations in units of molecule cm^{-3}. [b] From the measured sum and the yield for NO_3, the yields for Cl can be calculated. [c] Average value.

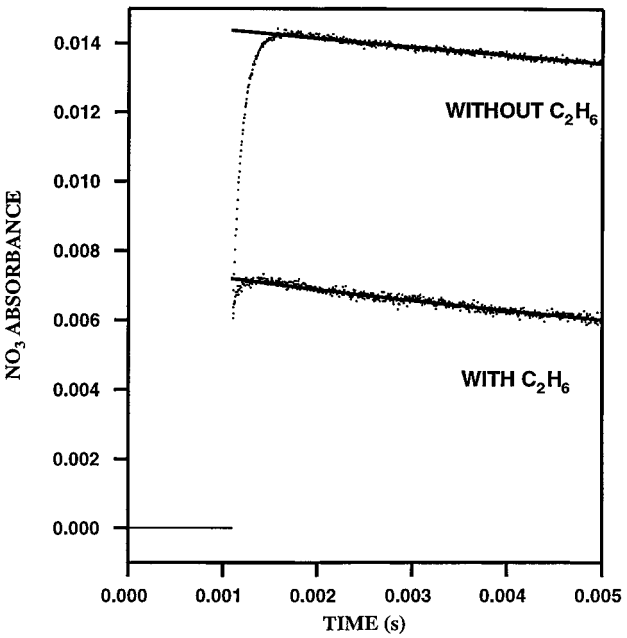

Figure 4. Typical NO_3 temporal profile following 248 nm photolysis of $ClONO_2$ in the presence of excess O_2, 209 Torr, without and with 17 Torr of C_2H_6. The solid lines are fits to the data used to extrapolate the absorption signal to the time of the laser pulse t_0.

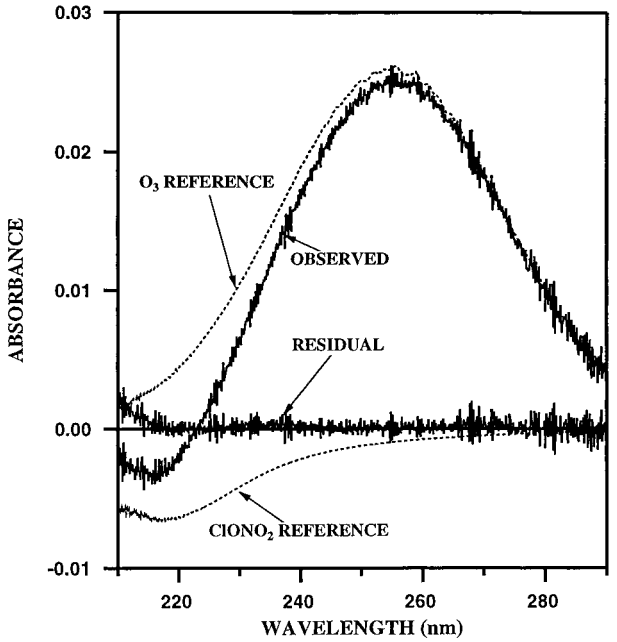

Figure 5. Diode array absorption spectrum recorded 15 ms following 193 nm photolysis of $ClONO_2$. Also shown are the O_3 and $ClONO_2$ reference spectra subtracted and added to the measured spectrum respectively to obtain the residual spectrum shown. The change in $ClONO_2$ determined in this way was used to calculate the absolute NO_3, Cl, and O quantum yields.

concentration upon photolysis. Even under these conditions, the scattered light from the laser entering the monochromator prevented measurements for ~20 μs following the photolysis pulse. The procedures and data analysis were the same as in the case of 308 nm.

Figure 4 shows the temporal variation of the absorbance profile at 661.9 nm, attributed to NO_3, in the presence of 7.5 Torr C_2H_6 and 134.4 Torr of O_2 in the cell. Even at the highest levels of Cl and O atom scavengers used, 17 Torr C_2H_6 and 209 Torr O_2, a rise of ~10% in the NO_3 absorption was observed following the laser pulse. This rise cannot be due to the reactions of Cl or O atoms with $ClONO_2$ because it did not change with the concentration of $ClONO_2$. This slow rise is attributed to the production of vibrationally excited NO_3 in the photolysis of $ClONO_2$ and the subsequent quenching to the ground vibrational state by the gases in the cell. In these experiments, the postmaximum NO_3 signal decayed with a first-order rate constant of ~45 s^{-1}, faster than that observed in either 351 and 308 nm photolysis experiments. Figure 5 also shows the NO_3 temporal profile with C_2H_6 removed from the photolysis mixture. As with the analysis of the 308 nm photolysis data, such measurements allowed us to determine the sum of the NO_3 and Cl yields.

The data analysis procedures were the same as in 308 nm photolysis. The NO_3 signals were analyzed to extract the initial value of $[NO_3]$. The average value of the NO_3 quantum yield was 0.60 ± 0.06 (Table 3). The measured quantum yield did not change significantly with the variation of the $ClONO_2$ concentration by a factor of 5 and the laser power by a factor of ~1.5. In the absence of C_2H_6, the sum of the quantum yields for NO_3 and Cl, $\Phi(NO_3 + Cl)$, was ~1.2; this value is double that of the NO_3 yield.

O atoms generated in the photolysis of $ClONO_2$ were scavenged by O_2 to produce O_3 *via* reaction 3 and quantified by measuring the concentration of O_3 produced *via* absorption at 278 nm. The absorption at long times, 20 ms after the laser pulse, was used to determine $[O_3]$. At these long times, reactive species such as $C_2H_5O_2$ and ClO were expected to be depleted *via* reactions and, hence, most of the measured absorption was expected to be due to O_3. As noted later, even at such long times, radicals such as ClO and $C_2H_5O_2$ were still present and could have contributed to the measured absorption (see Discussion). In these experiments, C_2H_6 was not present so that the ethyl peroxy radical could not have contributed to the measured absorption. The temporal profile of the absorbance at 278 nm showed a decay at early times consistent with the removal of ClO radicals followed by a relatively constant absorbance. Limiting the O_3 absorption measurements to 278 nm, due to interference from the laser pulse, severely limited the sensitivity of this measurement. The maximum absorbance signals were ~0.005 with an uncertainty of ± 0.002. Two measurements were made, Table 3, with an average O atom yield of ~0.3. Because we cannot be sure that there were no other species absorbing at 278 nm, this yield is quoted as an upper limit of <0.4. It does suggest a significant production of O atoms in the 248 nm photolysis of $ClONO_2$. More accurate values of this yield are presented in the companion paper.

193 nm Photolysis. Unlike measurements at 352.5, 308, or 248 nm, actinometry experiments were not necessary. The absorption cross section of $ClONO_2$ at 193 nm is such that the fraction of the $ClONO_2$ that was photodissociated could be measured precisely. Therefore, the only assumption made in determining the quantum yields is that the measured decrease in $ClONO_2$ concentration equals the concentration of $ClONO_2$ that absorbed light.

The fraction of $ClONO_2$ that was dissociated by the photolysis pulse was measured using the diode array detector and a shutter that could be opened at predetermined times before and after the laser pulse. The acquisition times were set such that a spectrum was acquired before the laser pulse and again beginning 15 ms after the laser pulse. The spectrum recorded before the laser pulse was used as the reference spectrum I_o to measure the changes in the composition in the cell following the laser pulse. A representative diode array spectrum is shown in Figure 5 along with the reference O_3 and $ClONO_2$ spectra subtracted from the measured spectrum. The residual spectrum

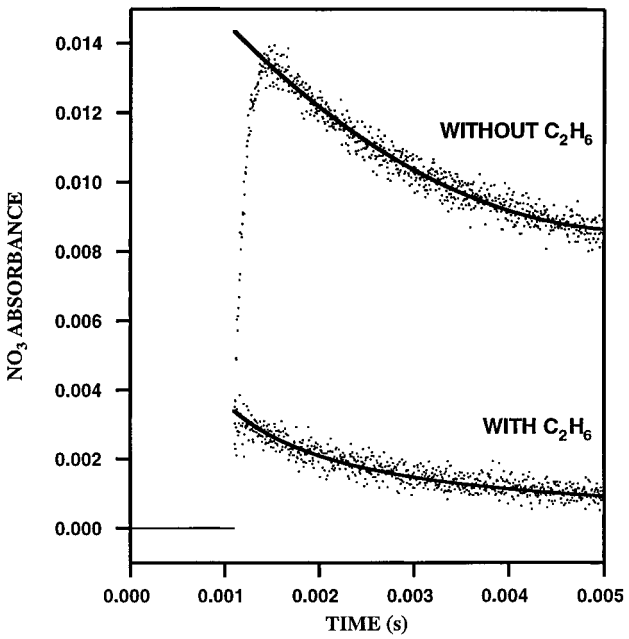

Figure 6. Typical NO_3 temporal profile following 193 nm photolysis of $ClONO_2$ in the presence of excess O_2 with and without C_2H_6.

obtained after subtracting O_3 and adding $ClONO_2$ is zero within the uncertainty of the measurement. The concentration of $ClONO_2$ whose spectral contribution had to be added is the concentration of $ClONO_2$ that was photolyzed, $\Delta[ClONO_2]$.

Figure 6 shows an absorption profile for NO_3 measured following 193 nm photolysis of a mixture of $ClONO_2/C_2H_6/O_2$ in N_2. The NO_3 quantum yield was extracted from the measured NO_3 signal and the measured concentration of $ClONO_2$ that was photolyzed,

$$\Phi_{NO_3}^{193} = \frac{[NO_3]_0}{\Delta[ClONO_2]} \qquad \text{(VI)}$$

Such measurements were carried out three times and yielded an average value of 0.18 ± 0.01.

The Cl atom yield was determined by measuring the NO_3 signal in the absence of C_2H_6 but with O_2 present, as in the experiments carried out at 248, 308, and 352.5 nm. The secondary slow increase in the NO_3 is attributed to the reaction of Cl atoms with $ClONO_2$. One such measured profile is shown in Figure 6. Upon the assumption that the only source of Cl atoms in this measurement is $ClONO_2$ photolysis, the Cl atom yield was measured to be 0.58. Note that the contributions of Cl_2 and OClO impurities to the Cl atom production are insignificant because the absorption cross section of $ClONO_2$ at 193 nm is much larger than that of either Cl_2 or OClO, unlike at 308 or 352.5 nm.

The quantum yields for Cl and O atoms were also determined by allowing these atoms to react with $ClONO_2$ and measuring the change in $ClONO_2$ using a diode array spectrometer after their reactions had gone to completion. To measure the Cl atom quantum yields, the amount of $ClONO_2$ photolyzed was first measured by using a mixture of $ClONO_2$, C_2H_6, and O_2 in N_2. Then, a mixture of $ClONO_2$ and O_2 was photolyzed. In the latter experiment, each photolytically generated Cl atom destroyed one $ClONO_2$. After the reactions of Cl atoms had gone to completion, the change in $ClONO_2$ concentration was measured and attributed to Cl atoms. A rough estimate of the O atom quantum yield was obtained by photolyzing a mixture of $ClONO_2$ and N_2 such that any O atoms that were formed could react with $ClONO_2$. Under these conditions, in addition to O atoms, Cl atoms and/or other free radicals could contribute to the $ClONO_2$ loss. Ten such measurements were performed from which a representative data set is given in Table 4. The quantum yield values obtained were 0.88 for O atoms and 0.45 for Cl atoms.

The quantum yield for O atoms was also measured by converting it to O_3 *via* its reaction with O_2. A mixture of $ClONO_2$, C_2H_6, and O_2 in N_2 was photolyzed and the change in absorption at 253.7 nm was measured using the monochromator/PM tube. Figure 7 shows a temporal absorption profile from one such experiment. At early times, <0.002 s after the laser pulse, the absorption signal shows a rapid decay, suggesting the presence of one or more reactive species. This early transient absorption is most likely due to ClO and/or $C_2H_5O_2$ formed following the photolysis. This rapid decay was also observed in the absence of C_2H_6, indicating that it may be due to ClO. A fraction (<20%) of the O_3 produced results from O_2 photolysis. The production of O_3 from O_2 photolysis was measured in a separate experiment in which only O_2 was photolyzed. The O_2 photolysis showed a fast rise to a stable absorption within ~100 μs, and no rapid decay of the absorption signal was observed. The O_3 produced in the $ClONO_2$ experiment was corrected for the O_3 production from O_2 photolysis. The O atom yield was measured four times with C_2H_6 present

TABLE 4: Quantum Yields for Production of NO_3, Cl, and O Atoms in the 193 nm Photolysis of $ClONO_2$ and the Experimental Conditions Used

$ClONO_2$ photolysis									
$P(C_2H_6)$ (Torr)	$P(O_2)$ (Torr)	P(total) (Torr)	$[ClONO_2]$ (10^{15})	$\Delta[ClONO_2]$ (10^{11})	$\Delta[NO_3]$ (10^{11})	$\Delta[O_3]$ (10^{11})	yield of NO_3	yield of Cl	yield of O
3.2	29	613	0.654	295	55		0.186		
3.0	30	617	0.757	300	53.7		0.179		
3.2	28	613	0.576	287	49.8		0.174		
							0.18 ± 0.01[b]		
1.3	25	616	0.460	211		160			0.76
1.8	26	617	0.460	224		194			0.87
1.5	25	608	0.471	209		193			0.92
1.5	25	617	0.469	219		197			0.90
3.0	30	617	0.757	300		262			0.87
									0.86 ± 0.12[b]
1.8	25	617	0.470	224					
1.8	0	617		421					0.88
0	0	617		522				0.45 ± 0.08	
3.3	29	613	0.654	295	55				
0	29	613	0.654	295	230			0.58	

[a] All concentrations in units of molecule cm^{-3}. [b] Average value.

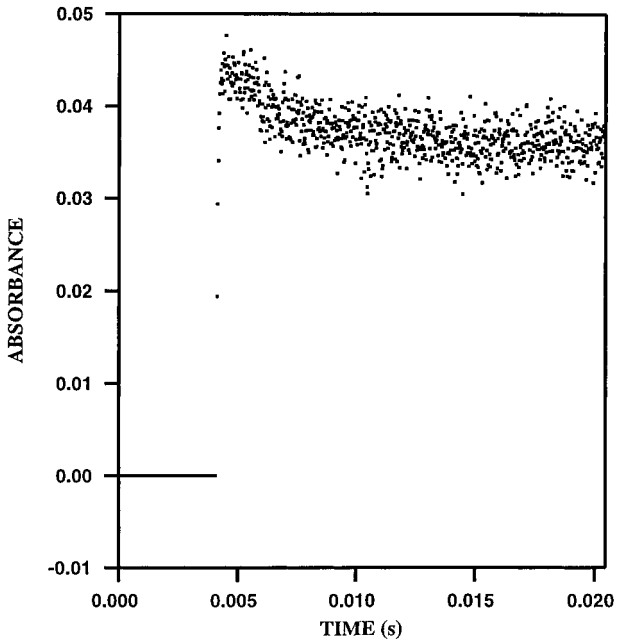

Figure 7. Absorbance profile at 253.7 nm following $ClONO_2$ photolysis at 193 nm.

giving 0.86 ± 0.06. A single measurement without C_2H_6 gave an O atom yield of 0.97.

The contributions of radicals such as ClO and $C_2H_5O_2$ to the measured O_3 production, and hence, the quantum yield of O atoms need to be assessed. The measured temporal profile of the 253.7 nm absorption showed little change after 5 ms. Considering the concentration of $ClONO_2$ that was dissociated, the concentrations of the photoproducts should be low. In the experiments carried out in the presence of C_2H_6 and O_2, the concentrations of radicals such as $C_2H_5O_2$ and ClO must be much less than the concentration of $ClONO_2$ that was photolyzed (*i.e.*, $<5 \times 10^{13}$ molecule cm^{-3} in 193 nm photolysis and $<1 \times 10^{13}$ molecule cm^{-3} at other wavelengths). Under these conditions, the self-reaction of $C_2H_5O_2$ will lead to a decrease of <4% in its concentration in 5 ms. During the first 5 ms, the loss of ClO due to its self reaction will be less than 10%. Removal of $C_2H_5O_2$ would be due mostly to its reactions with ClO, NO, and NO_3. Similarly, the loss of ClO will be controlled by reactions with $C_2H_5O_2$, NO_3, or NO. These loss processes may lead to a decrease of ~40% in the concentration of the radicals. Therefore, the contribution of these radicals to the measured absorption at 253.7 or 278 nm would be significant even if it appears that absorption is not changing with time. Further, molecular products such as ClONO and $ClNO_2$ could contribute to the measured absorption. The laser fluence during these measurements were high, but at most 5% of $ClONO_2$ in the cell was photolyzed. Therefore, the contribution from sequential photolysis of a primary photoproduct (which could be excited) to the measured absorption, and attributed to O_3, was small. For example, ClO produced by $ClONO_2$ photolysis could be further photolyzed by the same laser pulse to generate Cl and O atoms. At 248 nm, depending on the laser fluence, at most 5% of the observed O and Cl atoms could be due to photolysis of ClO photoproduct. Such a sequential photolysis will be even less important at 308 nm because of much lower absorption cross sections of the photoproducts. If the sequential photolysis was an important source of Cl atoms, the concentration of NO_3 produced *via* the $Cl + ClONO_2$ reaction would be larger than that from photolysis. As shown in Figure 4, the yield of NO_3 in the presence of the Cl atom scavenger was one-half that in its absence. Yet, conservatively, the quantum yields determined by monitoring UV absorption should be considered upper limits. The companion paper reports directly measured quantum yields for O atoms and those results are preferred.

A summary of the quantum yield results from this study are given in Table 5. The quoted uncertainties include the precision of the measurements and the estimated systematic errors, which are discussed below. The precision of the measurements was reflected by the standard deviation of the mean of a large number of measurements.

Discussion

In this study, we identified NO_3 as a direct product of $ClONO_2$ by measuring the absorption spectrum of NO_3 following $ClONO_2$ photolysis using a diode array spectrometer. In one set of measurements, subsequent to the fluence determinations, a mixture of $ClONO_2$, C_2H_6, and N_2 was photolyzed while keeping the laser fluence unchanged. A shutter was opened 15 ms after the laser pulse for ~2 ms, and a spectrum was measured using the diode array in the wavelength region of 620 to 690 nm. Using the spectrum of the cell contents taken prior to the photolysis pulse as a reference, the change in the spectrum after photolysis was calculated. The measured difference spectrum was the characteristic absorption spectrum of NO_3. There were no other significant absorptions in this region. This measurement clearly showed that NO_3 was a photoproduct of $ClONO_2$ and that absorption changes measured at 661.9 nm were due mostly, if not only, to NO_3. Further, the yield of NO_3 was measured by probing it at wavelengths where its absorption cross sections were 20 and 90% of the peak value; the same yields were measured. Therefore, the absorptions measured at 661.9 nm must be due entirely to NO_3. The contribution of NO_2 to the measured absorption at 661.9 nm is negligible even if photolysis of $ClONO_2$ produced 100 times as much NO_2 as NO_3.

If the NO_3 radical is produced in an electronically excited state, it is possible for it to dissociate before it is collisionally quenched. However, because the lower vibrational levels of the first excited state fluoresce and they can be quenched to the ground electronic state by collisions, their formation would be included in the NO_3 yield that is measured. Similarly, low vibrational levels of the ground electronic state will be quenched and detected. Thus, the reported quantum yield for NO_3 includes those for the production of some of the vibrationally excited ground state and electronically excited molecules.

The errors quoted in Table 2 are the standard deviations of the means of multiple experiments and, hence, represent the precision of the measurements. The other factors that add to the uncertainties in the measured quantum yields are the systematic errors. In this study, the sources of systematic errors are (1) the uncertainties in the absorption cross section of NO_3 at 661.9 nm, estimated to be <5% at 298 K; (2) the fluence of the laser; and (3) the UV absorption cross sections of $ClONO_2$ at the photolysis wavelength. As noted in our companion paper[1] and the Appendix, the systematic error due to the measurement of $[ClONO_2]$ is small. This is because the concentrations were determined by UV absorption and the absorption cross sections enter into the calculation of the concentration of $ClONO_2$ as well as the number of molecules which absorbed the photolysis light. Therefore, unless the measured absorption cross sections have systematic errors that vary with wavelength, they cancel in the calculation of the quantum yields. We estimate this error to be less than 2%. In calculating the laser fluence, we used reference photolytes whose absorption cross sections and photodissociation quantum yields are well-known. Therefore, we assume the total uncertainty in the quantum yields to be less than 16 at the 95% confidence level by assuming them to

TABLE 5: Summary of Quantum Yields in the Photolysis of $ClONO_2$ at 298 K and Recommended Values from Our Studies

	quantum yields						
λ (nm)	Cl	$O(^3P)$	NO_3	ClO	ClONO	NO_2	notes
260−380	1.0 ± 0.2	0.1	0.8−0.4	0.04			*b*
249			0.85−0.45				*c*
254		0.24	1.0−0.4		1.0−0.3		*d*
193	0.64 ± 0.08		0.64 ± 0.08	0.36 ± 0.08		0.36 ± 0.08	*e,f*
248	0.54 ± 0.08		0.54 ± 0.08	0.46 ± 0.08		0.46 ± 0.08	*e,f*
308	0.67 ± 0.06		0.67 ± 0.06	0.33 ± 0.06		0.33 ± 0.06	*e,g*
>200			0.31 ± 0.20	0.61 ± 0.2			*h*
>300			0.56 ± 0.08	0.44 ± 0.08			
193	0.53 ± 0.10†	0.38 ± 0.08*i*		0.29 ± 0.20*i*			
	0.45 ± 0.08	<0.9	0.18 ± 0.04*j*				
	0.58						
248	0.41 ± 0.13†	<0.10*i*		0.39 ± 0.19*i*			*k*
	0.60 ± 0.12	<0.4	0.60 ± 0.09				
308	0.64 ± 0.20†	<0.05*i*		0.37 ± 0.19*i*			
	0.73 ± 0.14		0.67 ± 0.09				
352.5			0.93 ± 0.24				
	Preferred Values from This and the Companion Work[a]						
193	0.5	0.4	>0.2	0.3			
222	0.40	0.17		0.60			
248	0.60	<0.10	0.60	0.40			
308	0.65	<0.05	0.65	0.35			
352.5			0.93				

[a] The quantum yields for Cl and O atoms from the companion paper are preferred over those deduced here. The quantum yield for NO_3 directly measured here are preferred. The quoted uncertainties are at the 95% confidence level and included estimated systematic uncertainties. [b] Chang *et al.*[21] Mass spectrometry. [c] Marinelli and Johnston.[15] Laser absorption. [d] Burrows *et al.*[22] Molecular modulated spectroscopy with UV−vis absorption and matrix isolation with FTIR. [e] The authors measured the ratio of the yields for ClO and NO_2 to Cl and NO_3. In this table, they have been converted to absolute quantum yields by assuming that these are the only two channels and that the quantum yield for the dissociation is unity. [f] Minton *et al.*[16] molecular beam/mass spectrometry. [g] Moore *et al.*[17] molecular beam/mass spectrometry. [h] Nickolaisen *et al.*[2] visible absorption spectrometry with broad-band photolysis. [i] Work from our laboratory: from the companion paper.[1] [j] This is a lower limit since a fraction of the NO_3 may have dissociated before it could be stabilized. [k] This work.

be independent of each other (see Appendix). We have included the estimated systematic uncertainties in our measured values of the quantum yields in Table 5.

The measured quantum yields were independent of the initial $ClONO_2$ concentration, varied over a factor of 7, photolysis laser fluence, varied over a factor of 3, and total pressure of N_2 and O_2 bath gases, varied from 120 to 620 Torr. NO_3 quantum yields measured at 352.5 nm photolysis were also found to be independent of temperature between 298 and 220 K, within the precision of our measurements.

The NO_3 quantum yield decreased with decreasing photolysis wavelength, $\Phi(NO_3) = 0.93$ at 352.5 nm to 0.18 at 193 nm. The Cl atom quantum yield was in a 1:1 correspondence with the NO_3 quantum yield with the exception of the measurements at 193 nm. In the 193 nm photolysis, the Cl atom quantum yield was 2.9 times larger than the NO_3 quantum yield. A possible explanation for this difference is the generation of NO_3 radicals that are sufficiently excited to undergo decomposition. The observed increase in the O atom yield is consistent with such a process. Evidence for the internal excitation of the NO_3 radical was also observed in the 248 nm photolysis measurements. At 248 nm a small secondary rise in the NO_3 absorption signal was observed in the presence of Cl and O atom scavengers, Figure 4. NO_3 was monitored using the 0−0 transition at 661.9 nm so that relaxation of excited NO_3 into the ground state would be observed as an increase in the absorption signal. However, the rise is slower than relaxation rates for NO_3* observed in the photolysis of N_2O_5.[14] Similar secondary increases in the NO_3 absorption signal were observed by Marinelli and Johnston[15] who employed 248 nm photolysis. Secondary reactions which form NO_3 are possible, but seem unlikely. The reaction of a photolysis product with $ClONO_2$ to form NO_3 would require a rate constant twice that for reaction 2 to account for the observed rise. Also the observed rise was independent of the initial $ClONO_2$ concentration. Reactions between photolysis products would be too slow to account for the observed rise. This secondary rise was not observed at any other photolysis wavelength.

The O atom yields were indirectly determined following $ClONO_2$ photolysis at 193 and 248 nm. Significant O atom yields were observed at both photolysis wavelengths. The O atoms could have formed as a direct photolysis product, *via* the decomposition of excited NO_2 or NO_3 photofragments, or the sequential photolysis of a primary photoproduct (see above). Our measurements could not discriminate between these processes. Our O atom yield measurements at 193 nm were complicated by O atom generation from O_2 photolysis and contributions of other absorbers to the measured yield.

The NO_3 absorption signal decayed following its production in all experiments. The decay rate was smallest following 308 nm photolysis; the pseudo-first-order rate constant for NO_3 loss was $<5\ s^{-1}$. The fastest decay rate was observed with 193 nm photolysis followed by 248 nm photolysis and then finally 352.5 nm photolysis. NO is the only possible photolysis product which is not scavenged and reacts rapidly with NO_3. The observed decay rates can be interpreted in terms of the NO generated as a photolysis product. The observed NO_3 decay rate at 352.5 nm can be almost completely accounted for by the NO formed by photolysis of an NO_2 impurity. The observed first-order decay of NO_3 for 352.5 nm photolysis, shown in Figure 3, is $\sim 15\ s^{-1}$. The upper limit for the NO reaction based on our estimates of the NO_2 impurity level would be $\sim 5\ s^{-1}$, if expressed as a first-order loss. The absence of NO_3 decay in the 308 nm photolysis is consistent with this interpretation because the photolysis of the NO_2 impurity would be insignificant at this wavelength. The NO yields implied from the observed decay of NO_3 produced in the 193 and 248 nm photolysis fall in the range 0.2 to 0.3. However the estimated yield was sensitive to the amount of NO_3 formed. In the experiments carried out in the presence of C_2H_6, an average

value of 0.33 ± 0.01 was obtained. However in the absence of C_2H_6, where twice as much NO_3 was produced, the NO_3 decay rate remained the same. The reason for this is unclear.

In the companion paper,[1] we have compared the quantum yield for the production of Cl and O atoms and of ClO with those from previous studies and this work. The quantum yields of Cl and O atoms in this work were determined somewhat indirectly and could have small contributions from other species. The formation of NO_3 with a time constant consistent with the loss of Cl atoms *via* reaction 2 adds to our confidence in assigning the rise to Cl atoms. Further, the secondary rise was completely suppressed when 4 Torr of C_2H_6 was added to the cell. Since Cl atoms react rapidly with C_2H_6, and O atoms do not, we can be confident that very little of the measured secondary rise was due to O atoms. The quantum yields for O atoms were derived by observing absorption changes at 253.7 or 278 nm. Therefore, they are much less reliable; absorptions due to species other than O_3 could have contributed to these yields. The NO_3 yields measured here are to be preferred over those deduced in the companion paper. The Cl and O atom yields reported in the companion paper are preferred over those deduced here. Table 5 lists the values of the quantum yields from our two studies. It also list the values we prefer. The preferred values were selected after evaluating interference, uncertainties, and methods used to obtain the quantum yields.

We compare our results of the quantum yields for the production of NO_3 radical with those previously measured and suggest that the major photodissociation pathway for $ClONO_2$ photolysis in the stratosphere is to give NO_3 radical and Cl atom. Table 5 lists the previously measured quantum yields for various products in studies where the quantum yields for NO_3 were also deduced or measured. The picture that emerges from the post-1990 studies is that NO_3 is a major product of $ClONO_2$ photolysis at all wavelengths. The study that was most similar to ours was that by Marinelli and Johnston,[15] and their results at 249 nm agree with our results. (Note that these authors also used a KrF laser, but they quote the wavelength as 249 nm.) The quantum yields for Cl atoms reported in the companion paper are in rough agreement with the yields of NO_3, the coproduct of Cl, except at 193 nm. At this short wavelength, the channel to produce Cl + O + NO_2 is energetically feasible and is consistent with the production of Cl and O being high, while that of NO_3 is low. However, directly measured yields of O atoms are much less than what is inferred from this study.

ClO is also an important photoproduct. This observation is a confirmation of the results of recent investigations.[2,16,17] The sums of the yields of Cl and NO_3 are similar at 248 and 308 nm and the sum of the yields of Cl and ClO are close to 1. Thus, it appears that the primary photolysis pathways are reactions 1a and 1b. As the wavelength increases, the yield of NO_3 also increases while that of ClO decreases. Thus channel 1b appears to increase at the expense of other channels as the wavelength increases. Therefore, the most likely set of products in the stratosphere are NO_3 and Cl. This is the same recommendation as that made by DeMore *et al.* in 1992[18] and in 1997.[10] On the basis of our measured values at 298 K as well as at temperatures close to 220 K, we can be confident that greater than 70% of the photolysis leads to NO_3 production at wavelengths close to 350 nm. Between 308 and 351 nm, reaction 1a is also significant.

Nickolaisen *et al.*[2] have reported that the quantum yield for the loss of $ClONO_2$ decreases with increases in pressure based partly on the decrease in quantum yields of products with increase in pressures. Their experiments were carried out using a broad-band light source and, hence, as noted by Nickolaisen *et al.*, the quantitative implications of their findings to the atmosphere is difficult. We have not measured the quantum yield for the loss of $ClONO_2$ (except at 193 nm) but the production of NO_3. Our measurements were carried out at pressures of 100 to 325 Torr, which is close to or greater than the pressures (and number densities) encountered in the stratosphere. The bath gas in most of these experiments was predominantly O_2. Further, our measured yield at 352.5 nm did not change with temperature. These observations show that the quantum yield for the photodissociation of $ClONO_2$ in the stratosphere, at least up to 352.5 nm, will be greater than 0.7 and is likely to be 1. The calculated *J*-value for the photodissociation of $ClONO_2$ as a function of wavelength at 15 km and 40° and 55° N are shown in Figure 8. The region that emphasizes the longest wavelengths is the wintertime high latitude lower stratosphere. It is clear that >50% of $ClONO_2$ photolysis at 40° N and >45% at 55° N in the winter takes place at wavelengths less than 352.5 nm. Therefore, the photodissociation rate of $ClONO_2$ in any part of the stratosphere cannot be less than 50% of the currently recommended values, which assume unit quantum yield for the dissociation. The fractional contribution by wavelengths less than 352.5 nm will be larger during other seasons.

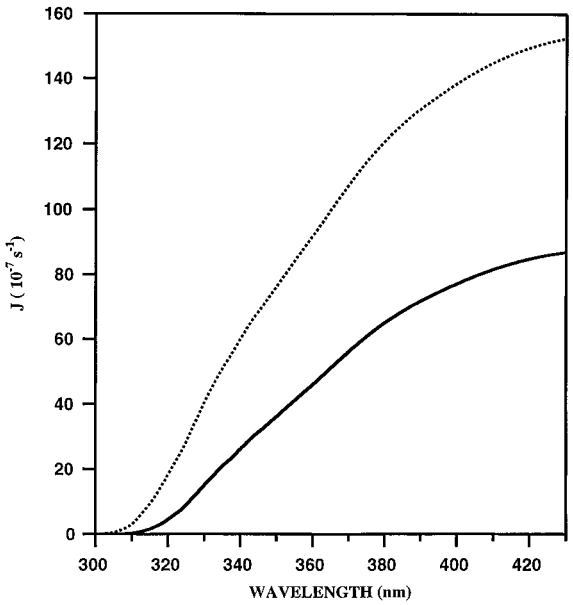

Figure 8. Integrated photodissociation rate constants, *J*-values, for photolytic loss of $ClONO_2$ at 40° N (dashed line) and 55° N (solid line) in the winter.

The quantum yield for the production of NO_3 is not unity between 308 and 352.5 nm. If we assume that the quantum yield for ClO is 0.4 and that for NO_3 is 0.6 between 308 and 352.5 nm, the efficiency of the catalytic cycle involving $ClONO_2$ is

$$ClO + NO_2 \xrightarrow{M} ClONO_2 \quad (14)$$

$$ClONO_2 \xrightarrow{h\nu} Cl + NO_3 \quad (1b)$$

$$NO_3 \xrightarrow{h\nu} NO + O_2 \quad (15)$$

$$Cl + O_3 \rightarrow ClO + O_2 \quad (16)$$

$$NO + O_3 \rightarrow NO_2 + O_2 \quad (17)$$

$$\text{Net: } 2\,O_3 \rightarrow 3\,O_2 \quad (18)$$

which destroys ozone in the stratosphere, will be approximately 60% of that calculated by assuming the quantum yield for NO_3

to be 1. We could not determine the quantum yield for reaction 1c. However, on the basis of the measured yields for ClO, Cl, and NO_3, the yield for reaction 1c is likely to be <0.3. If this channel occurs, the catalytic efficiency for ozone destruction will be greatly enhanced because it completely bypasses the photolysis of NO_3, which yields NO and O_2 less than 10% of the time.[10] Therefore, it would be useful to measure the quantum yield for channel 1c directly and for channel 1b near 400 nm.

Acknowledgment. We thank L. Hollberg of NIST for generous assistance with the diode lasers and Stuart McKeen for providing the solar fluxes. This work was funded in part by the Upper Atmospheric Research Program of the National Aeronautics and Space Administration.

Appendix

The equations which relate the quantum yield of NO_3 with the measured quantities are

$$\Phi_{NO_3}^{352.5} = \frac{[NO_3]}{F_\lambda [ClONO_2] \sigma_{ClONO_2}^{352.5}} \qquad \text{(IV)}$$

$$F_{352.5} = \frac{\Delta[Cl]}{2[Cl_2]\sigma_{Cl_2}^{352.5}} \qquad \text{(A1)}$$

$$[NO_3] = \frac{A_{661.9}}{\sigma_{NO_3}^{661.9} l} \qquad \text{(III)}$$

The Cl concentration was measured by reacting Cl with O_3 and measuring the change in absorption at 253.7 nm, which is attributed to the sum of the loss of ozone and formation of ClO (see text). When all these parameters are included in eq IV, it is reduced to

$$\Phi_{NO_3}^{352.5} = 2(\sigma_{O_3}^{253.7} - \sigma_{ClO}^{253.7}) \frac{1}{\sigma_{NO_3}^{661.9}} \left(\frac{\sigma_{Cl_2}^{352.5}}{\sigma_{Cl_2}^{330}} \right) \times \left(\frac{\sigma_{ClONO_2}}{\sigma_{ClONO_2}^{352.5}} \right) \frac{A_{NO_3}^{661.9} \quad A_{Cl_2}^{330} \quad (1 + e^{-A_{352.5}(ClONO_2)})}{A_{ClONO_2} \Delta A^{253.7} \quad (1 + e^{-A_{352.5}(Cl_2)})} \qquad \text{(A2)}$$

This equation includes a collection of absorption cross sections and a collection of measured absorbances or changes in absorbances. Often, ratios of absorption cross sections of the same compound at different wavelengths appear. In that case, we assume that the systematic errors cancel since we take the cross sections from the same study. We further assume the errors in terms 1, 2, 3, and 4 to be 5, 5, 2, and 2%, respectively, at 67% confidence level. The uncertainties in the measured absorbances are given by the precision and the lower limit for ability to measure the absorbance. This limit depends on the method of measurement. This uncertainty is approximately 0.05% for diode array measurements, 0.02% for the monochromator/PMT measurements, and 0.005% for the diode laser measurement. Propagating these errors in quadrature leads to an estimate of the systematic uncertainty in the measured value of the NO_3 quantum yield of 16% at the 95% confidence level. Similar expressions are derived for other wavelengths.

References and Notes

(1) Goldfarb, L.; Schmoltner, A.-M.; Gilles, M. K.; Burkholder, J. B.; Ravishankara, A. R. *J. Phys. Chem.* **1997**, *101*, 6658−6666.
(2) Nickolaisen, S. L.; Sander, S. P.; Friedl, R. R. *J. Phys. Chem.* **1996**, *100*, 10165−10178.
(3) Burkholder, J. B.; Mauldin, R. L., III; Yokelson, R. J.; Ravishankara, A. R. *J. Phys. Chem.* **1993**, *97*, 7597−7605.
(4) Yokelson, R. J.; Goldfarb, L.; Burkholder, J. B.; Gilles, M. K.; Ravishankara, A. R. *J. Phys. Chem.* **1994**, *99*, 13976−13983.
(5) Yokelson, R. J.; Burkholder, J. B.; Fox, R. W.; Talukdar, R. K.; Ravishankara, A. R. *J. Phys. Chem.* **1994**, *98*, 13144−13150.
(6) Trolier, M.; Mauldin, R. L., III; Ravishankara, A. R. *J. Phys. Chem.* **1990**, *94*, 4896−4907.
(7) Mauldin, R. L., III Kinetics and Photochemistry of Halogen Oxides Relevant to the Stratosphere. Ph.D. Thesis, University of Colorado, 1991.
(8) Mauldin, R. L., III; Burkholder, J. B.; Ravishankara, A. R. *J. Phys. Chem.* **1992**, *96*, 2582−2588.
(9) Wieman, C. E.; Hollberg, L. *Rev. Sci. Instrum.* **1991**, *62*, 1−20.
(10) DeMore, W. B.; Sander, S. P.; Golden, D. M.; Hampson, R. F.; Kurylo, M. J.; Howard, C. J.; Ravishankara, A. R.; Kolb, C. E.; Molina, M. J. Chemical Kinetics and Photochemical Data for Use in Stratospheric Modeling, Evaluation No. 12. JPL Publication 97-4; Jet Propulsion Laboratory: Pasadena, CA, 1997.
(11) Schmeisser, M. *Inorg. Synth.* **1967**, *9*, 127.
(12) Molina, L. T.; Molina, M. J. *J. Geophys. Res.* **1986**, *91*, 14501−14508.
(13) Wahner, A.; Tyndall, G. S.; Ravishankara, A. R. *J. Phys. Chem.* **1987**, *91*, 2734−2738.
(14) Ravishankara, A. R.; Wine, P. H.; Smith, C. A.; Barbone, P. E.; Torabi, A. *J. Geophys. Res.* **1986**, *91*, 5355−5360.
(15) Marinelli, W. J.; Johnston, H. S. *Chem. Phys. Lett.* **1982**, *93*, 127−132.
(16) Minton, T. K.; Nelson, C. M.; Moore, T. A.; Okumura, M. *Science* **1992**, *258*, 1342−1345.
(17) Moore, T. A.; Okumura, M.; Tagawa, M.; Minton, T. K. *Faraday Discuss. Chem. Soc.* **1995**, *100*, 295−307.
(18) DeMore, W. B.; Sander, S. P.; Golden, D. M.; Hampson, R. F.; Kurylo, M. J.; Howard, C. J.; Ravishankara, A. R.; Kolb, C. E.; Molina, M. J. Chemical Kinetics and Photochemical Data for Use in Stratospheric Modeling, Evaluation No. 10. JPL Publication 92-20; Jet Propulsion Laboratory: Pasadena, CA, 1992.
(19) Burkholder, J. B.; Bair, E. J. *J. Phys. Chem.* **1983**, *87*, 1859−1863.
(20) Burkholder, J. B.; Talukdar, R. K.; Ravishankara, A. R. *Geophys. Res. Lett.* **1994**, *21*, 585−588.
(21) Chang, J. S.; Barker, J. R.; Davenport, J. E.; Golden, D. M. *Chem. Phys. Lett.* **1979**, *60*, 385−390.
(22) Burrows, J. P.; Tyndall, G. S.; Moortgat, G. K. *J. Phys. Chem.* **1988**, *92*, 4340−4348.
(23) Nelson, C. M.; Moore, T. A.; Okumura, M.; Minton, T. K. *Chem. Phys.* **1996**, *207*, 287−308.